Separation Science and Technology
Publication details, including instructions for authors and subscription information:
http://www.informaworld.com/smpp/title~content=t713708471

CO_2 Capture Using Activated Amino Acid Salt Solutions in a Membrane Contactor

Jian-Gang Lu[a]; Yan Ji[a]; Hui Zhang[a]; Min-Dong Chen[a]
[a] School of Environmental Science & Engineering, Nanjing University of Information Science & Technology, Nanjing, China

Online publication date: 02 June 2010

To cite this Article Lu, Jian-Gang , Ji, Yan , Zhang, Hui and Chen, Min-Dong(2010) 'CO_2 Capture Using Activated Amino Acid Salt Solutions in a Membrane Contactor', Separation Science and Technology, 45: 9, 1240 — 1251
To link to this Article: DOI: 10.1080/01496391003775865
URL: http://dx.doi.org/10.1080/01496391003775865

Separation Science and Technology, 45: 1240–1251, 2010

ISSN: 0149-6395 print/1520-5754 online
DOI: 10.1080/01496391003775865

Taylor & Francis
Taylor & Francis Group

CO_2 Capture Using Activated Amino Acid Salt Solutions in a Membrane Contactor

Jian-Gang Lu, Yan Ji, Hui Zhang, and Min-Dong Chen
School of Environmental Science & Engineering, Nanjing University of Information Science & Technology, Nanjing, China

An activated solution based on amino acid salt was proposed as a CO_2 absorbent. Piperazine (PZ) was selected as an activating agent and added into the aqueous glycine salt to form the activated solution. A coupling process, which associated the activated solution with a PP hollow fiber membrane contactor, was set up. An experimental and theoretical analysis for CO_2 capture was performed. The performances of CO_2 capture by the coupling process were evaluated using the PZ activated solution and the non-activated glycine salt solution. A numerical model for the simulation of the hollow fiber membrane gas–liquid mass transfer was developed. Typical parameters such as outlet gas phase CO_2 concentration, capture efficiency, and mass transfer coefficient for the activated solution were determined experimentally. The effects of operation temperature and liquid CO_2-loading on mass transfer coefficient and capture efficiency were discussed in this work. Axial and radial concentration profiles of CO_2 in the fiber lumen and mass transfer flux were simulated by the model. Results show that the performances of the PZ activated glycine salt solution are evidently better than that of the non-activated glycine salt solution in the membrane contactor for CO_2 capture. Elevation of the operation temperatures can enhance the overall mass transfer coefficient. The activated solution can maintain higher capture efficiency especially in the case of high CO_2-loadings. The gas phase CO_2 concentration with the activated solution is lower than that with the non-activated solution whether along axial or radial distances in the fiber lumen. The model simulation is validated with experimental data.

Keywords activated solution; amino acid salt; carbon dioxide; membrane contactor; model and simulation; piperazine

INTRODUCTION

Carbon dioxide (CO_2) is generally considered as one of the main causes that result in the greenhouse effect and global warming (1). It is responsible for intensive human activities such as the combustion of fossil fuels as the primary energy source that have caused the concentration of greenhouse gases in the atmosphere to rise significantly over the last 200 years (2). It has turned to be a worldwide issue to reduce CO_2 emission and decrease CO_2 concentration in the atmosphere; the capture of CO_2 from the industrial sources seems to be an important measure for this issue. Therefore, low energy-consumption, available, efficient technologies have attracted significant attention for the capture and removal of CO_2 from gas mixtures produced by industrial sources. Current separation and capture technologies based on a variety of physical and chemical processes include absorption, adsorption, conversion, cryogenic separation, and membrane techniques (3) and other novel methods (4).

Membrane-based gas-liquid process, namely membrane gas absorption (MGA), is a coupling process that combines the conventional technique of gas absorption into solvents and a membrane contactor as a mass-transfer device. MGA has the advantages of both membrane contactor and gas absorption processes. The membrane contactor furnishes a known high specific surface area, independent control of gas and liquid flow rates, and a compact and energy efficient device (5), while the gas absorption provides a high selectivity and a high driving force for mass transfer. MGA has been considered to be a promising alternative to conventional and potential large-scale application technology for the recovery and removal of CO_2 (6).

Development of MGA for CO_2 capture has been over 20 years since Cussler initially studied the field of MGA [7]. Relevant studies on MGA for CO_2 capture have been in progress rapidly (8–15). The studies mostly deal with those investigations involving the mass-transfer performances, the effects of operating conditions, membrane configuration, and module structure on absorption flux and mass-transfer coefficients, models for mass transfer, mass-transfer kinetics, and various efficient liquid absorbents. Aqueous amino acid salts as a type of novel absorbents for MGA have been regarded as favorable absorbents which provide both of high active reaction with CO_2 and compatibility with membrane (i.e., friendly to membrane, difficult to wet the micropores unlike alkanolamines) (8). In addition, aqueous amino acid salts

Received 9 July 2009; accepted 8 February 2010.
Address correspondence to Jian-Gang Lu, School of Environmental Science & Engineering, Nanjing University of Information Science & Technology, Ninliulu 219 Pukouqu, Nanjing 210044, China. Tel.: +86 25 58731090; Fax: +86 25 58731089. E-mail: jglu@nuist.edu.cn

are non-toxic, thermally stable, regenerative, commercially available, and low vapor pressure. The development of absorbents is vital to MGA. High performance absorbents have especially attracted the significant attention of researchers. Recently, the blended absorbents (also called complex absorbents) which usually are composed of two single absorbents (e.g., alkanolamines) in varying compositions have been presented by numerous researchers in order to improve the performances of absorbents for CO_2 capture (11,14,16–18). The formulation of blended absorbents is based on the principle that it combines the favorable characteristics of different single absorbents while suppressing their unfavorable characteristics (14). The characteristics include, for instance, a higher absorbing capacity, a higher absorption rate, a lower energy consumption, a lower corrosion, a lower oxidative degradation and good chemical compatibility with membrane. The blended absorbents can combine the advantages of single absorbents in the blends. As a rule, one component in the blended absorbent is as an activating agent (or called as an additive) to be added into another component as a main solvent. Here, the blended absorbent is also called the activated absorbent/solution. The main solvent is usually large in varying compositions compared with the additives. Product costs of the additives are generally higher than the main solvent. For example, piperazine (PZ) or 2-Amino-2-methyl-1-propanol (AMP) is added into methyldiethanolamine (MDEA) as a main solvent to form the MDEA-based blended absorbent (or called as the activated MDEA solution) (11). PZ has a special molecular structure in which a symmetrical diamino cyclic structure exists. PZ has been confirmed to be an efficient activating agent in blended absorbents for CO_2 capture (11,19). However, amino acid salts as main solutes in the blended absorbents are seldom investigated in existing literature.

In this paper, CO_2 capture from a CO_2/N_2 mixture was investigated by coupling of an activated amino acid salt solution and a polypropylene (PP) hollow fiber membrane contactor. PZ was selected as an activating agent and added into aqueous glycine salt (GLY) to form the activated solution. Effects of various factors on mass transfer of the membrane contactor were studied. The experimental results were compared between the activated and non-activated solution. Reaction mechanisms and activations of PZ are discussed theoretically. A mathematical model is developed for the mass transfer of the membrane contactor associating with the activated solution for CO_2 capture.

THEORY

Reaction Mechanism

The reaction mechanism of amino acid salts reacting with CO_2 is considered as the zwitterionic mechanism which is similar to primary and secondary amines (8,20). Following reactions occur in the solution:

$$2^{-}OOCRNH_2 + CO_2 \rightleftharpoons {}^{-}OOCRNHCOO^{-} + {}^{-}OOCRNH_3^{+} \quad (1)$$

$$^{-}OOCRNH_3^{+} \rightleftharpoons {}^{-}OOCRNH_2 + H^{+} \quad (2)$$

From the zwitterionic mechanism of Eqs. (1) and (2), a conclusion can be deduced that if a base (B) is added into the solution, B will coalesce with $H^+ : B + H^+ \rightleftharpoons BH^+$. The equilibriums of Eqs. (1) and (2) will move right because of the dissipated H^+ in the solution. Well then, the reaction of amino acid salts with CO_2 will be accelerated. So, a suitable compound as additive can be selected to satisfy the B. The reaction of amino acid salts with CO_2 (Eq. (1)) will be accelerated theoretically.

When PZ as an activating agent is added into the aqueous amino acid salt, the following reactions may occur in the system:

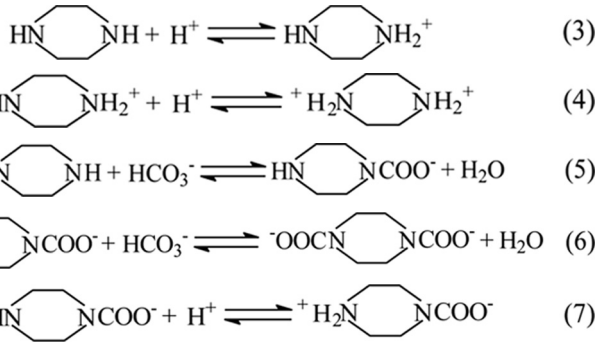

(3)

(4)

(5)

(6)

(7)

As a mild base B, PZ and its products may serve to catalyze proton extractions in the reaction mechanism. For a complex solution mixed with PZ, the activation of PZ can be explained by a homogeneous activation mechanism (14,21). Meanwhile, PZ can also react with CO_2 as a secondary amine. The reaction of CO_2 with PZ can be regarded as the rapid pseudo-first-order reaction in parallel with that of CO_2 with the main amine in the solution (22,23).

In addition, in the aforementioned system of reactions, CO_2 also reacts with the hydroxide ions present in solution:

$$CO_2 + OH^{-} \rightleftharpoons HCO_3^{-} \quad (8)$$

As a single amino acid salt solution (e.g., potassium glycinate), the contribution of the reaction of Eq. (8) to the overall reaction rate can be considered negligible because aqueous amino acid salt is a weak base (19). However, when an additive (e.g., PZ) is presented in amino acid salts solution, the contribution of the reaction of Eq. (8) to the overall reaction rate cannot be negligible because the basicity of the amino acid salts solution is enhanced as well as present as shown in Eqs. (5) and (6) in the solution.

Based on the zwitterionic mechanism and assuming the second proton transfer step considered irreversible owing to catalytic actions of the additive, the overall reaction rate of CO_2 with the amino acid salt can be expressed in the presence of homogeneous catalysis of PZ according to the chemical reaction mechanism as (11,14):

$$R_{ov} = k_{ov}C_{CO_2} = k_G C_{GLY} C_{CO_2} + k_P C_{PZ} C_{CO2} + k^*_{OH^-} C_{OH^-} C_{CO_2} = (k_G C_{GLY} + k_P C_{PZ} + k^*_{OH^-} C_{OH^-}) C_{CO_2} \quad (9)$$

Accordingly, the overall reaction rate constant k_{ov} has the following expression:

$$k_{ov} = k_G C_{GLY} + k_P C_{PZ} + k^*_{OH^-} C_{OH^-} \quad (10)$$

The parameters k_G, k_P and $k^*_{OH^-}$ in Eqs. (9) and (10) can be calculated in the following equations (24–26):

$$k_G = 2.24 \times 10^{16} \exp\left(-\frac{8544}{T}\right) \exp(0.44 C_{GLY}) \quad (11)$$

$$k_P = 5.8 \times 10^4 \exp\left[-\frac{3.5 \times 10^4}{R}\left(\frac{1}{T} - \frac{1}{298}\right)\right] \quad (12)$$

$$\log_{10} k^*_{OH^-} = 13.635 - \frac{2895}{T} \quad (13)$$

Mass Transfer in the Membrane Contactor

In a membrane contactor for gas absorption, the gas and liquid phases flow on opposite sides of the membrane in a countercurrent fashion. CO_2, that is contained in the gas mixture, crosses the hydrophobic microporous membrane and enters the liquid phase. With the non-wetting operation mode, the gas preferentially fills the membrane pores to meet minimal membrane resistance (15). Figure 1 describes the mass-transfer regions, dominant resistances, and flow configuration in a membrane contactor. The mass-transfer process consists of three consecutive steps:

1. diffusion of a gaseous component i ($i = CO_2$) from the gas phase bulk to the outer surface of the membrane;
2. diffusion through membrane pores to the gas-liquid interface; and
3. dissolution into the liquid film (i.e., liquid-boundary layer) and then chemical reaction/liquid-phase diffusion, eventually into the liquid phase bulk.

Thus, the overall mass-transfer process consists of three resistances in series: the gaseous phase boundary layer ($1/k_g$), the membrane ($1/k_m$), and the liquid phase boundary layer ($1/k_L$). The overall mass-transfer resistance ($1/K$) can be expressed as Eq. (14) in a resistance-in-series model based on the fiber outer wall. The mass-transfer flux (J_i) of component i is given as Eq. (15) based on the driving force of concentration differences.

$$\frac{1}{Kd_o} = \frac{1}{k_g d_{in}} + \frac{1}{k_m d_m} + \frac{1}{H k_L d_o} \quad (14)$$

$$J_i = k_g(C_{i,g} - C_{i,g,mem}) = k_m(C_{i,g,mem} - C_{i,g,int}) = k_L(C_{i,L,int} - C_{i,L}) = K\Delta C_i \quad (15)$$

where K is the overall mass transfer coefficient; k_g, k_m, and k_L are individual mass-transfer coefficients of the gas side, the membrane, and the liquid side, respectively. The variable H represents the Henry's coefficient of CO_2 between the gas and liquid phases. For chemical absorption, $k_L = Ek^\circ_L$; E is the enhancement factor due to chemical reaction, and k°_L is

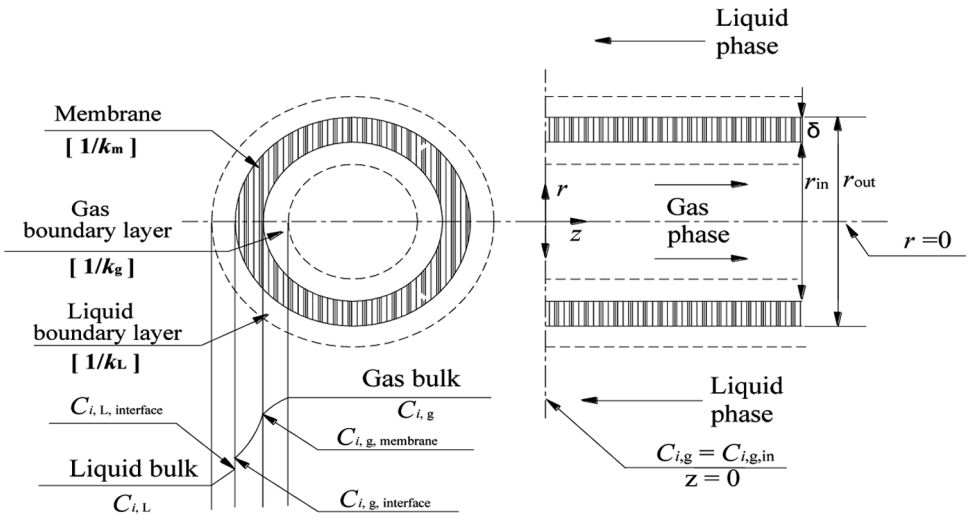

FIG. 1. Mass transfer regions, dominant resistances and flow configuration in MGA.

the physical mass-transfer coefficient. d_{in}, d_o, and d_m are the inner fiber diameter, the outer fiber diameter, and the logarithmic mean average diameter, respectively. $C_{i,g}$, $C_{i,g,mem}$, $C_{i,g,int}$, $C_{i,L,int}$, $C_{i,L}$, and ΔC_i are the concentration of CO_2 in the gas bulk, at the interface of the gas and the membrane, at the gas side of the gas/liquid interface, at the liquid side of the gas/liquid interface, in the liquid bulk, and logarithmic mean value, respectively.

Mathematical Model

On the basis of the case of the gas mixture in the lumen of a hollow fiber membrane and the liquid on the shell side, as described schematically in Fig. 1, and by combining the solution properties, membrane and module geometric characteristics, and process conditions, the following assumptions are presented:

i. steady operation state and isothermal conditions exist;
ii. Newtonian fluids with constant physical properties and axis-symmetry are used;
iii. ideal gas behavior and obedience of Henry's law are exhibited;
iv. equilibrium exists at the gas–liquid interface;
v. fully developed laminar flow occurs in the lumen; and
vi. negligible radial convection and axial diffusion also occur.

With these assumptions and the resistance-in-series concept, a mathematical model is developed to describe the absorption of a gas into a liquid flowing through a membrane hollow fiber in MGA. The differential equation of the model based on a mass balance can describe the CO_2 concentration profile in the lumen, and the equation is given as:

$$u_z \frac{\partial C_{i,g}}{\partial z} = D_{i,g}\left[\frac{1}{r}\frac{\partial}{\partial r}\left(r\frac{\partial C_{i,g}}{\partial r}\right)\right] \tag{16}$$

where $D_{i,g}$ is the CO_2 diffusion coefficient in the gas phase and u_z is the gas axial velocity inside the lumen. In a laminar flow and fully developed velocity profile, u_z can be described with the following equation:

$$u_z = 2\bar{u}\left[1 - \left(\frac{r}{r_{in}}\right)^2\right] \tag{17}$$

where $\bar{u}$ is the average gas velocity in the lumen and r_{in} is the inner radius of the fiber. With the initial conditions for the differential equation Eq. (16),

$$C_{i,g} = C_{i,g,in}, \quad \text{for } z = 0 \text{ and all } r \tag{18}$$

$$\frac{\partial C_{i,g}}{\partial r} = 0, \quad \text{for } r = 0 \text{ and all } z \tag{19}$$

where $C_{i,g,in}$ is the concentration of CO_2 at the inlet of the gas phase. At the membrane–liquid interface, the flux of CO_2 is equal to its flux in the gas phase, namely, mass is conserved with respect to CO_2. Thus, the boundary condition exists

$$D_{i,g}(\partial C_{i,g}/\partial r) = K_{ext}(mC_{i,L} - C_{i,g}), \quad \text{for } r = r_{in} \text{ and all } z \tag{20}$$

where K_{ext} is the external (membrane wall and shell side) mass transfer coefficient. K_{ext} is a combination of the mass-transfer coefficients of both the liquid phase and the membrane, and is expressed as:

$$\frac{1}{K_{ext}} = \frac{1}{k_m} + \frac{1}{Hk_L} = \frac{1}{k_m} + \frac{1}{HEk_L^o} \tag{21}$$

To obtain the value of K_{ext}, the parameters of Eq. (21) need to be determined. The membrane mass-transfer coefficient, k_m, is calculated by the following equation deduced by Fick's law,

$$\frac{1}{k_m} = \frac{\tau\delta}{D_{i,m}\varepsilon} \tag{22}$$

where τ, δ, and ε are the tortuosity of the membrane pore, the thickness of the membrane wall, and the porosity, respectively. The tortuosity for Eq. (22) can use the Wakao-Smith equation, $\tau = 1/\varepsilon$. Where $D_{i,m}$ is the CO_2 diffusion coefficient in the membrane pores. CO_2 diffusion behavior in membrane gas-filled pores depends on the pore size and the molecule average free path. For a binary gas mixture with a micron-size pore size at atmospheric pressure, the diffusion behavior is a combination of molecular and Knudsen diffusion (27). Equation (23) can characterize the combination for the parameter of $D_{i,m}$.

$$\frac{1}{D_{i,m}} = \frac{1}{D_{i,g}} + \frac{1}{D_k} \tag{23}$$

The following correlation is available for the physical mass transfer coefficient k_L° (28), which can satisfy the conditions of the module used in this work, for example, hydrophobic membrane, parallel-flow, $0 < Re < 500$, packing fraction $0.04 < \varphi < 0.4$, etc.

$$Sh = \frac{k_L^o d_h}{D_{i,L}} = 5.85(1-\varphi)\left(\frac{d_h}{L}\right)Re^{0.6}Sc^{0.33} \tag{24}$$

where *Sh, Re*, and *Sc* are the Sherwood number, the Reynolds number, and the Schmidt number, respectively. L, d_h, and φ are the effective length of the membrane, the hydrodynamic diameter $(=(D_{in}^2 - nd_o^2)/nd_o$, D_{in} is the shell inner diameter, n the number of fibers, and d_o is the

fiber inner diameter) and packing fraction of the module, respectively. CO_2 diffusion coefficient in the liquid phase, $D_{i,L}$, can be given below as (29):

$$D_{i,L}\mu^{0.54}/T = 6.109 \times 10^{-8} \quad (25)$$

where μ is the viscosity of the solution. The calculation of the enhancement factor, E, uses the conventional mass-transfer model which has been validated to be applicable for MGA (5,8,11,14). A detailed explanation for E can be found in the literature (30,21). E is given by the following:

$$E = \frac{-Ha^2}{2(E_\infty^* - 1)} + \sqrt{\left[\frac{Ha^2}{4(E_\infty^* - 1)^2} + \frac{E_\infty^* Ha^2}{E_\infty^* - 1} + 1\right]} \quad (26)$$

Based on the penetration model, the asymptotic infinite enhancement factor, E_∞^* is defined as:

$$E_\infty^* = \left(1 + \frac{C_{a,in}D_a}{mC_{i,int}D_{i,L}}\right)\left(\frac{D_{i,L}}{D_a}\right)^{0.5} \quad (27)$$

where D_a is the amine diffusion coefficient in aqueous solution, and $C_{a,in}$ is the absorbent concentration at the liquid inlet of the module. D_a, is calculated by means of the Wilke-Chang relationship (32)

$$D_a = 3.06 \times 10^{-15} T/\mu \quad (28)$$

For the system of CO_2 reaction with amino-acid-salt-based complex absorbents, a modified Hatta number Ha can be given by:

$$Ha = \frac{\sqrt{k_{ov}D_{i,L}}}{k_L^o} \quad (29)$$

where k_{ov} is the overall reaction rate constant that can be calculated by Eq. (10) based on the reaction mechanism and the conditions at the location of the liquid outlet ($z = 0$).

According to concept of "mixing cup" concentration (33), the outlet gas concentration $C_{i,g,out}$ can be determined by

$$C_{i,g,out} = \frac{\int_0^{r_{in}} 2\pi r u_z C_{i,g} dr}{\int_0^{r_{in}} 2\pi r u_z dr} = \frac{\int_0^{r_{in}} C_{i,g} u_z r dr}{\int_0^{r_{in}} u_z r dr} \quad (30)$$

The Henry's coefficient, H, is estimated by the literature (24,34–36), the viscosity of the absorbents, μ, is determined experimentally. The values of the parameters of the hollow fiber membrane module used in model are listed in Table 1.

The numerical scheme for the model of the partial differential equations can be solved along with the initial and boundary conditions as well as the reaction kinetics based on a steady state. Discretization for the partial differential equation adopts the Euler equation. The initial and boundary conditions are accordingly transferred into an equation corresponding to the discrete function (11,14). The calculation values are gained using the Matlab program.

TABLE 1
Characteristics for the hollow fiber membrane module

Module inside diameter (mm)	32
Fiber outside diameter (μm)	500
Fiber inside diameter (μm)	300
Fiber wall thickness (μm)	100
Fiber length (mm)	200
Number of fibers	1800
Average pore size (μm)	0.2
Fiber porosity	0.60
Packing fraction (%)	9.60
Contactor area (outer, m^2)	0.56

EXPERIMENTAL

Experimental Unit and Procedures

Figure 2 is a schematic diagram of the experimental setup of the membrane contactor and gas absorption coupling for CO_2 capture. By turning the valve of the mixed-gas cylinder to the desired flow rate, the mixed-gas stream, through a gas flow meter and a water saturator, was fed into the fiber lumen of the end of the module at a pressure that was slightly lower than that of the liquid side to prevent the dispersion of gas bubbles into the liquid. The liquid absorbent was introduced by a gear pump from the solution tank, through a liquid-flow meter and a preheater, to the shell side of the module in a counterflow mode in the opposite direction as the gas stream. The liquid absorbent at the inlet of the module always maintained fresh, CO_2 in the gas mixture in the fiber lumen diffused through the membrane pores into the liquid in the shell side

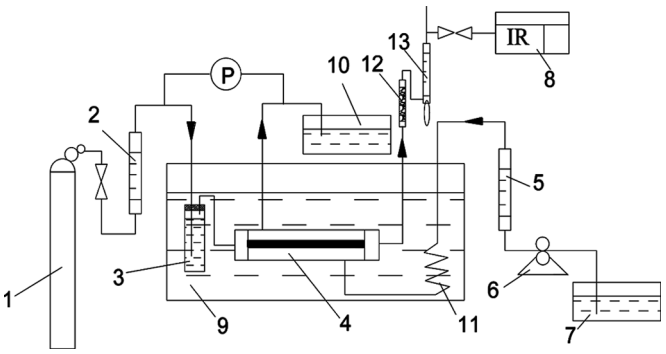

FIG. 2. Schematic diagram of experimental setup of a membrane contactor and gas absorption coupling for CO_2 capture. 1-Mixed-gas cylinder, 2, 5-Flowmeters, 3-water saturator, 4-Membrane contactor, 6-Gear pump, 7,10-Solution tank, 8-IR gas analyzer, 9-thermo water bath, 11-Preheater, 12-Drying column, 13-Soap film meter.

and was absorbed by the absorbent. The treated gas stream was released from another end of the module. The absorbent that contained CO_2 entered another solution tank. The membrane module was placed in a thermo water bath to be maintained at a constant temperature. Gas stream and the absorbent were preheated before entering the membrane module by the water saturator and the preheater. The mixed gas was prepared in a gas cylinder in laboratory by the method of mixing N_2 into CO_2 complying with the principle of partial pressure. The flow meters were calibrated beforehand. The experiment was continued for about 20 min to allow the system to reach steady state. Steady state conditions were indicated by a constant CO_2 concentration from an IR gas analyzer in the outlet gas stream of the module. Experiments were carried out at atmospheric pressure (0.1 MPa). The transmembrane pressure was maintained at 28–60 mmH_2O. A drying column was used to dry the treated gas stream. The soap film meter at the outlet gas stream was used to calculate the CO_2 mass conservation. The absorbent concentrations were the following: single amino acid salt solution, 1.0 kmol/m^3 glycine salt (GLY) (neutralized with equal mole KOH to form the glycine salt); activated solution, 0.75 kmol/m^3 GLY salt + 0.25 kmol/m^3 piperazine (PZ) (neutralized with KOH equal to the glycine mole). Other operation conditions were the following: the content of CO_2 in gas phase in about 10%, water bath at 20, 30, and 40°C, and gas and liquid flow rates at 0.05–0.1 m^3/h and 30–120 mL/min, respectively. The membrane module used in this work was equipped with a tube-shell parallel-flow structure, hydrophobic polypropylene hollow fiber membrane, and PVC material in the shell-side. The properties of the module (Tianjing Blue Cross Membrane Technology Co., China) are summarized in Table 1.

Materials and Methods of Analysis

In this work, N_2 and CO_2 were commercial cylinder gases and their purity was more than 99.99% (Nanjing Real Special-gas Co., China). The gas mixture was prepared in a gas-prepared system to a given concentration based on the partial-pressure principle. GLY was a biochemical reagent (Shanghai Chemical Co., China). The purity of PZ was 99.9% (Shanghai Chemical Co., China). The total amine concentration was determined by titration with a standard 0.1 kmol/m^3 sulfuric acid (H_2SO_4) solution using a methyl orange indicator. The content of CO_2 in the gas phase was analyzed by the IR gas analyzer (MB154S, Varian Co., USA) with reproducibility: ±1.5%. For the determination of the CO_2 content in the liquid phase, a known volume of the liquid sample was acidulated with a 1:4 ratio of a H_2SO_4 aqueous solution and the volume of the evolved gas was measured with a gas burette. After temperature and pressure corrections, the CO_2 content of the liquid sample was calculated (37). The error was ±0.02 mL.

Experimental Data Processing

In this work, capture efficiency η, overall mass transfer coefficient K, and mass transfer flux J_i are experimentally adopted to evaluate the performances of the activated solution in the membrane contactor.

Capture efficiency:

$$\eta = \frac{G_{\text{in}} C_{i,\text{g,in}} - G_{\text{ont}} C_{i,\text{g,out}}}{G_{\text{in}} C_{i,\text{g,in}}} \tag{31}$$

Mass transfer flux:

$$J_i = \frac{G_{\text{in}} C_{i,\text{g,in}} - G_{\text{out}} C_{i,\text{g,out}}}{A_{\text{m}}} \tag{32}$$

Overall mass transfer coefficient:

$$K = \frac{G_{\text{in}} C_{i,\text{g,in}-G_{\text{out}} C_{i,\text{g,out}}}}{A(\Delta C_{\text{n}})} \tag{33}$$

where G is the gas voluminal flow rate. A_{m} is available area for gas-liquid mass transfer of the membrane contactor ($=n\pi d_{\text{o}} L$). ΔC_{m} is the logarithmic mean driving force based on gas phase concentrations.

RESULTS AND DISCUSSION

Experimental Investigations of Typical Performances for Activated Solution and MGA

In order to evaluate the performances of the activated solution, experiments were performed using the setup of Fig. 2 with the activated and the glycine salt solution for MGA. The experimental data, expressed in a dimensionless form $C_{i,\text{g,out}}/C_{i,\text{g,in}}$ vs. liquid flow rates V_{L}, are presented in Fig. 3. The experimental results show that, CO_2

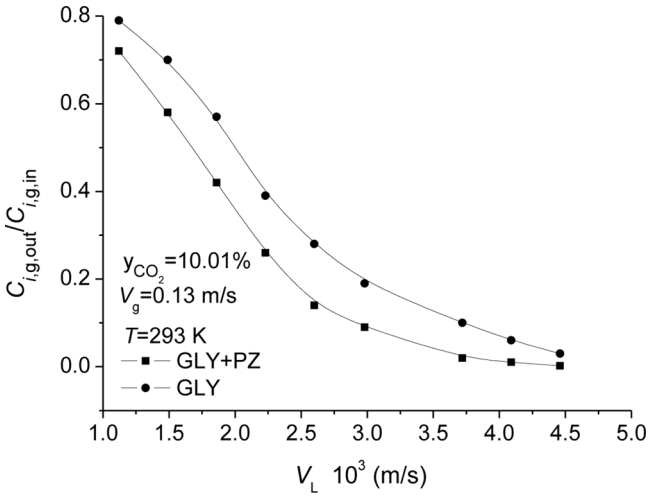

FIG. 3. Comparison of performance between GLY and GLY + PZ solution in the membrane contactor in a dimensionless form $C_{i,\text{g,out}}/C_{i,\text{g,in}}$ vs. liquid flow rate V_{L}.

concentration in the gas phase at the outlet of the module decreases with the increase of liquid flow rates. The CO_2 concentration of the outlet gas phase with the PZ activated solution is significantly lower than that with the single glycine salt solution, average low by 10–30% for the same operation conditions. Performance of the activated solution is evidently better than that of the single glycine salt solution in PP hollow fiber membrane contactor for CO_2 capture. It demonstrates that PZ can activate not only alkanolamines (e.g., MDAE) and inorganic salts (e.g., K_2CO_3) (11,14,19,21–23) but also amino acid salts. The activating effect of PZ on amino acid salts can be explained by the reaction mechanism in this wok. It is confirmed to be a high efficient activating agent and promotion effect for CO_2 capture in MGA. This good result suggests that in existing amine processes for CO_2 capture, as far as a smaller number of PZ would be added into the amines the content of CO_2 in the treated stream could be decreased not to change any conditions of the processes or technologies. Of course, further research is needed for usage on an industrial level with regard to the composite glycine salt solution activated by PZ.

Capture efficiency is one of the separation properties of MGA. The experiments were carried out with the activated solution for capture efficiency of MGA. The experimental results are given as Fig. 4. It can be found that the capture efficiencies increase with the increase of the liquid flow rates, while the efficiencies decrease with the increase of the gas flow rates. Capture efficiency can be obtained by more than 90%. Maximal capture efficiency can arrive at 99.9%. These results indicate the complex glycine salt solution activated by PZ is a high efficient absorbent for CO_2 capture. It is noticeable that capture efficiencies of MGA significantly depend on gas and liquid flow rates. The gas component CO_2 can adequately diffuse through the membrane pores at lower gas flow rates, while the liquid mass transfer resistance is sufficiently low at higher liquid flow rates and entering liquid fresh enough. So, higher capture efficiencies can be obtained at lower gas flow rates and higher liquid flow rates. Apparently, as for a given MGA process, there would be an optimal gas and liquid flow rates for a satisfactory capture efficiency in actual industrial applications.

Mass transfer coefficient is an important parameter for MGA. The experiments were conducted for the determination of the overall mass transfer coefficient with the activated and the non-activated solution. The results are shown in Fig. 5. It can be seen that, the overall mass transfer coefficient, K, increases with the increase of gas and liquid flow rates. For identical operation conditions, K with the activated solution is much higher than that with the non-activated solution. The average value of K with the activated solution is 1.3 times of that with the non-activated. In addition, the values of K increased with the liquid flow rates initially, and then almost reached a plateau. Apparently, alteration of operation parameters such as gas and liquid flow rates can promote the mass transfer of the membrane contactor, but the promotion is limited for MGA. This has been an accordant conclusion confirmed by numerous investigators. The enhancement of mass transfer relies essentially on the chemical reaction (i.e., reaction rate) (6,11,14). With a constant overall concentration of the activated absorbent, a small amount of activating agent (e.g., PZ) can significantly enhance the mass transfer of MGA by the information of Fig. 5. Wang et al. (9) investigated the CO_2 capture by three typical amines solutions using hollow fiber membrane contactors. The influence of the liquid flow rates on mass transfer of

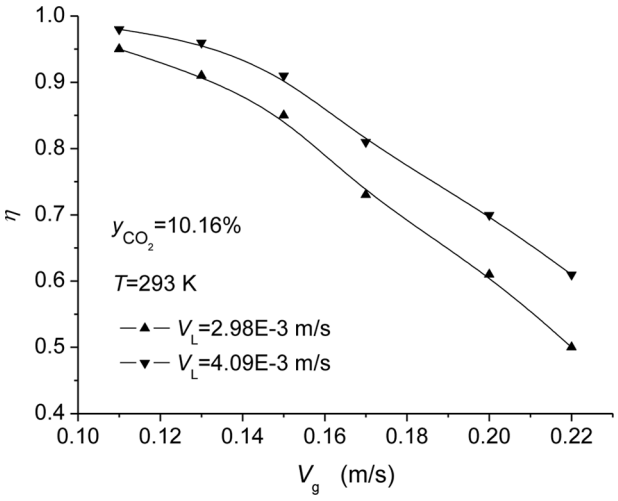

FIG. 4. Effect of flow rates s on capture efficiency with the activated solution.

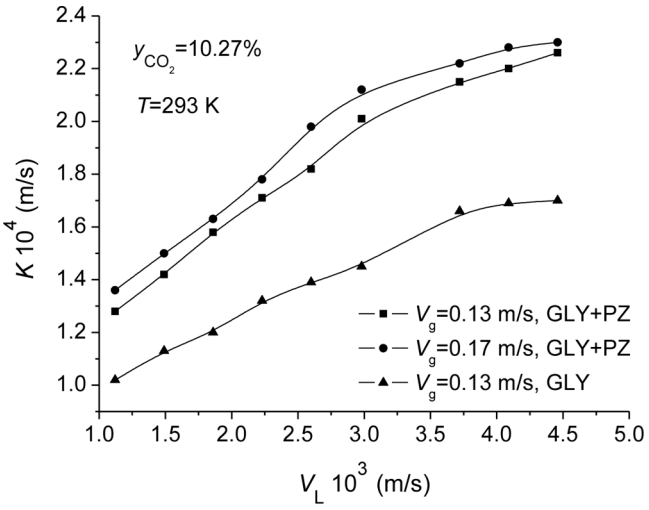

FIG. 5. Determination of overall mass transfer coefficient of the membrane contactor using GLY and GLY + PZ solution.

the membrane contactor by the MDEA solution was very small. However, the influences of the liquid flow rates on the mass transfer of the membrane contactor by both AMP and DEA solutions were very large. It was due to that the reaction rate of CO_2 with MDEA was much slower than that of AMP and DEA. In the same way, PZ present in the solution can intensively enhance the reaction rate of CO_2 with the activated solution.

Effect of Operation Temperature on Mass Transfer Coefficient

As a rule, the membrane contactors are operated at ambient temperatures. In actual application, seasonal temperatures can influence on the mass transfer of MGA. Experiments were carried out to investigate the effect of operation temperatures on the mass transfer coefficient using the activated solution at 293~313 K. Operation temperatures were controlled to reach a given constant temperature by the thermo water bath and less than 315 K considering the heat-resistant performance of the PP membrane. Experimental data are expressed as Fig. 6. The results show that, with the increase of operation temperatures, the overall mass transfer coefficients increase. The increase of operation temperatures enhances not only the components diffusion, but also the chemical reaction rate. Therefore, higher operation temperatures are in favor of the coupling operation of membrane contactor and gas absorption. Kumar and Dindore's work obtained the same results (8,38). Meanwhile, higher operation temperatures can avoid the crystallization of amino acid salts during CO_2 absorption, especially for the absorbents with high amino acid salts concentration at high CO_2 loading (39). Nevertheless, the operation temperatures cannot be elevated to reach a very high value. Operation temperatures cannot exceed the tolerated temperature of the membrane (i.e., heat-resistant limit temperature), or else would damage the structure of the membrane. Moreover, an increase of the operation temperatures can also result in the decrease of CO_2 solubility in the absorbent and the increase in the evaporation of the absorbent, which would decrease the drive force of mass transfer and increase the cost of the absorbent. Additionally, higher operation temperatures could induce the absorbent to wet membrane pores which could cause the instability of mass transfer of the contactor (15,40). Consequently, the selection of the operational temperature for the membrane absorption process is a compromise.

Effect of Liquid CO_2-Loading on Activation of PZ

The liquid CO_2-loading, α, is the quantity of CO_2 dissolved in the solution by both physical and chemical absorption. It can be expressed as moles of CO_2 per mole of amine in the solutions and indicated by the parameter α in this work. Experiments were performed to study the effect of CO_2-loadings on activation of PZ. Various CO_2-loadings of the solutions could be obtained by beforehand CO_2 absorption into the solutions to reach the given loadings. The experimental data, expressed in capture efficiency η versus α, are given in Fig. 7. The experimental results show that the capture efficiency η decrease with the increase of the CO_2-loadings in the inlet solutions. The downtrend of the curves in Fig. 7 with the activated solution is obviously lower than that with the non-activated solution. The higher the CO_2-loadings of the solutions, the larger the downtrend differences are. As the CO_2-loadings of the solutions increase to 0.32 mol/mol from zero, the capture efficiency of the non-activated solution decrease by 31.3%, while the capture efficiency of the activated solution only decrease by 18.6%. Thereby, the activated solution can maintain a higher capture efficiency.

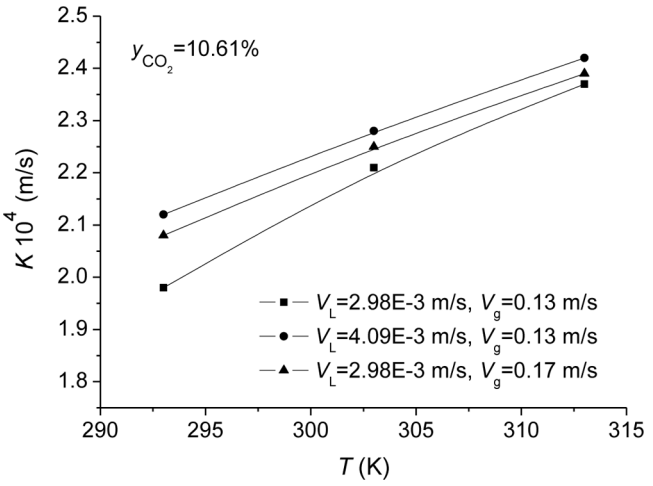

FIG. 6. Effect of operation temperatures on mass transfer coefficient using GLY + PZ solution.

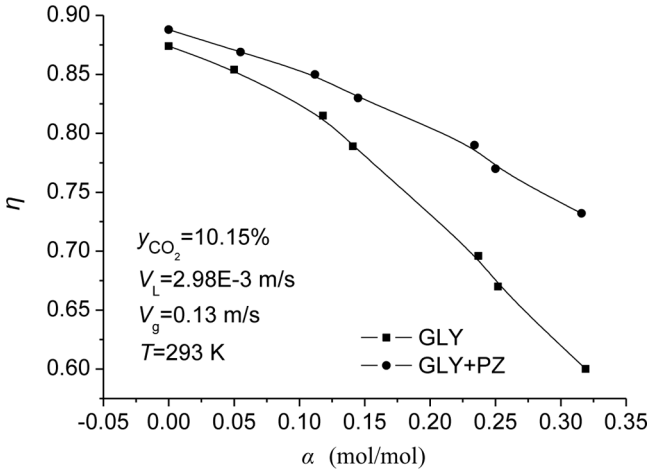

FIG. 7. Effect of liquid CO_2-loading on activation of PZ.

Especially in the case of high CO_2-loadings, the performances of the activated solution can display more effectively in comparison with non-activated solution. It is very significant in the actual application for the recovery of the high CO_2 concentration in flue gases such as coal-fired plants. Increased CO_2 loading leads to a reduction of the available free amines and hence reduction in the absorption rates. Capture efficiency generally increases with the amine concentrations (8,9).This is because of the increase of the active component in the liquid boundary layer with the amine concentration, which results in higher CO_2 solubility. When the activating agent PZ exists in the solution, the dissipation can be weakened ultimately (11). The reaction mechanisms can also account for the activation of PZ. In addition, a higher capacity of the activated solution can be obtained in comparison with that of the single solution. The capacity effectively increases the overall kinetics for mass transport.

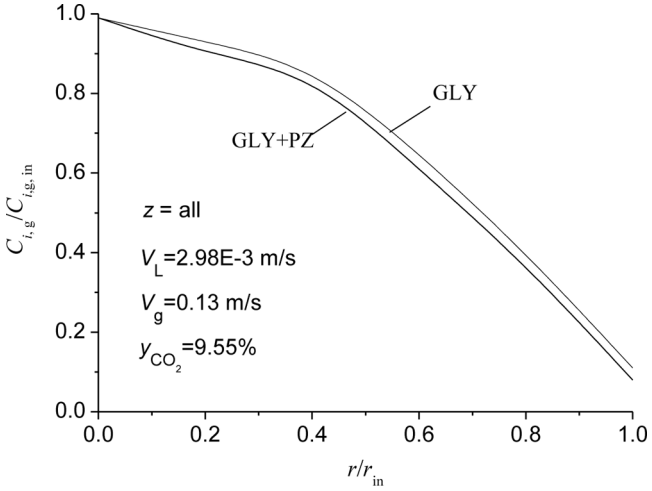

FIG. 9. Dimensionless CO_2 concentration of gas outlet vs. dimensionless radial distances at 293 K.

Comparison Between Experimental Results and Process Modeling

Axial and radial concentration profiles of CO_2 can characterize the distributions of CO_2 concentration in the lumen of the fiber. The model in this work can simulate them along dimensionless axial distances with various dimensionless radial distances, respectively. The results are given in Figs. 8 and 9. The simulation indicates that, the CO_2 concentration in the lumen decreases along the axial and radial distances of the fiber in the case of a steady laminar flow. At the same axial distance, the CO_2 concentration is much lower near the fiber wall than that at the center. The CO_2 concentration in the gas phase with the PZ activated solution is lower than that with the non-activated solution whether along axial or radial distances in the lumen of the fiber. The CO_2 concentration gradient in the lumen in the case of using the activated solution is larger than that in the case of using the non-activated solution. It demonstrates that the driving force for CO_2 transfer with the activated solution is larger than that with the non-activated solution under the same experimental conditions, and that, absorption is more efficiently promoted by the activating agent PZ. It suggests that efficient activating agents could significantly enhance the mass transfers of membrane contactors, and that, it would be important to develop novel activating agents for CO_2 capture of MGA. Additionally, the dimensionless CO_2 concentration at the membrane–gas interface ($r/r_{in} = 1.0$) where the gaseous phase boundary layer exists, is much lower than that at $r/r_{in} = 0.5$. This shows that in the three mass-transfer resistances in MGA for CO_2 capture using the amine solutions as absorbents, the resistance to the gas boundary layer cannot be neglected. Meanwhile, the trends of curves can be found that the effective fiber length has a considerable effect on outlet CO_2 concentrations. Because the residence time increases with the effective length of the fiber, the capture efficiency increases. Larger residence time is in favor of the adequate diffusion of CO_2 to reach chemical equilibrium. However, it is not reasonable that the longer the fiber or the larger the residence time, the greater the capture efficiency is. As CO_2 concentration at the wall reach a certain value that equals to that of chemical equilibrium, the capture efficiency no longer increases. Hereby, the fiber has a maximal effective length. The maximal effective fiber length should be predicted theoretically.

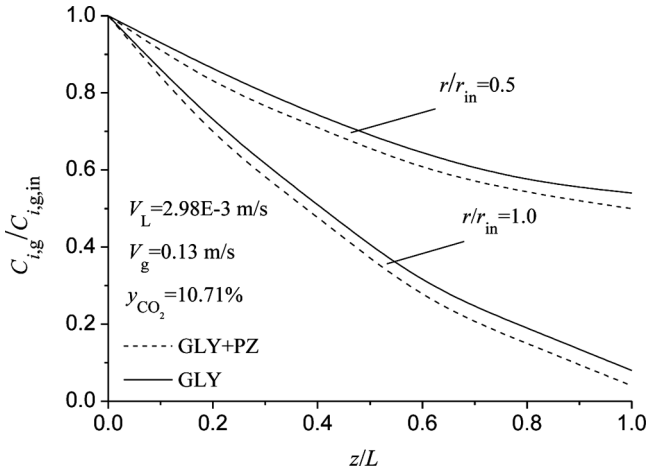

FIG. 8. Dimensionless CO_2 concentration vs. dimensionless axial distances at 293 K.

Figures 10 and 11 describe the simulation by the model as well as experiments with respect to the mass transfer flux. The results show that, first, the mass transfer fluxes increase with the increase of gas and liquid flow rates. The increase of gas and liquid flow rates can decrease the

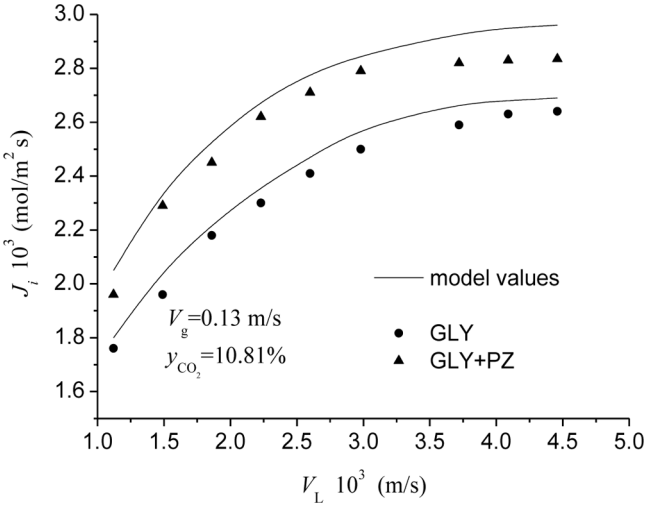

FIG. 10. Simulation of mass transfer with liquid flow rates at 293 K.

thicknesses of gas and liquid phase boundary layers. Accordingly, the resistances to gas and liquid sides decreases, the mass transfer fluxes increase. All researchers relating to MGA seem to observe this phenomena (5–16,27). However, it can be found that the curves of Fig. 11 are flatter than that of Fig. 10. This indicates that the effects of the gas flow rates on the fluxes are lower than that of the liquid flow rates in this work, and thus, the resistance to the gas phase boundary layer is smaller than that to the liquid phase boundary layer. Second, the mass transfer fluxes of PZ activated solution are larger than that of the non-activated glycine salt solution whether theoretically or experimentally. It suggests that adding a little amount of activating agent into an absorbent in the case of constant overall concentration, the mass transfer of MGA for CO_2 capture could be enhanced remarkably.

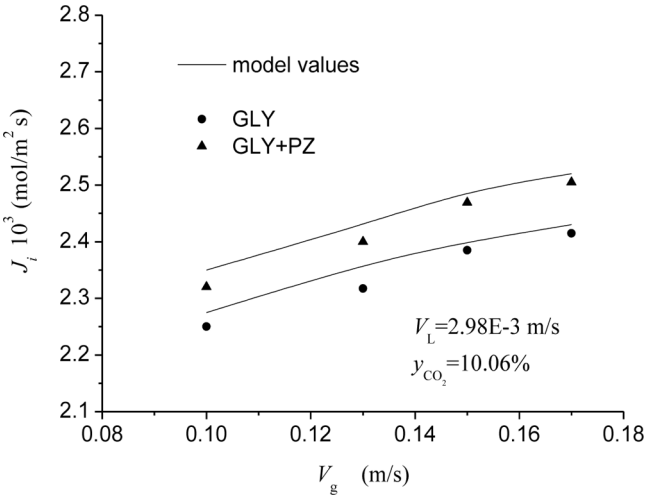

FIG. 11. Simulation of mass transfer with gas flow rates at 293 K.

This would effectively decrease the circulating capacity of the absorbent, and thus save energy in actual applications. Third, the model simulation is validated with experimental data. The average error is within 16.5%. The maximal error is less than 25%. In addition, the model values are higher than the experimental. The errors of activated solution are slightly larger than that of the non-activated solution. The causes for those are possibly slight partial wetting of membrane pores that is not considered in the model. The wetting of the activated solution is likely higher than that of the glycine salt solution because PZ as an amine added into the glycine salt solution resulted in the decrease of the surface tension of the solution. The partial wetting of the membrane pores from the activated solution will be further investigated in next work.

CONCLUSIONS

The performances of the PZ activated glycine salt solution are evidently better than that of the non-activated glycine salt solution in the PP hollow fiber membrane contactor for CO_2 capture. The outlet gas phase CO_2 concentration with the activated solution is significantly lower than that with the non-activated solution. The capture efficiency of MGA significantly depends on gas and liquid flow rates. Higher capture efficiency can be obtained at lower gas flow rates and higher liquid flow rates. The overall mass transfer coefficient, K, with the activated solution is much higher than that with the non-activated solution. The average value of K with the activated solution is 1.3 times of that with the non-activated solution. Operation parameters such as gas and liquid flow rates can limitedly promote mass transfer of membrane contactor. The enhancement of the mass transfer relies essentially on the chemical reaction. Higher operation temperatures are in favor of the coupling operation of the membrane contactor and gas absorption. However, the selection of the operational temperature is a compromise in order to avoid the damage of the membrane structure and the decrease of CO_2 solubility as well as the evaporation of absorbent. The downtrend of the capture efficiency with the activated solution is obviously lower than that with non-activated solution with the increase of the CO_2-loadings. The activated solution can maintain higher capture efficiency, especially in the case of high CO_2-loadings. The gas phase CO_2 concentration with the activated solution is lower than that with the non-activated solution whether along axial or radial distances in the fiber lumen with a steady laminar flow by simulation of the model. The driving force for CO_2 transfer with the activated solution is larger than that with the non-activated solution. Efficient activating agents could significantly enhance the mass transfers of membrane contactors. The model simulation is validated with experimental data. The average error is within 16.5%. The maximal error is less than 25%.

ACKNOWLEDGEMENTS

This work was supported by the University Natural Science Project of Jiangsu Province (09KJB610003) and the Science Research Fund of NUIST (20080315).

NOMENCLATURE

A_m	mass transfer area of the membrane contactor (m^2)
C	concentration ($kmol\,m^{-3}$)
$\triangle C_i$	concentration logarithmic mean value ($kmol\,m^{-3}$)
d	fiber diameter (μm or m)
D	diffusion coefficient (m^2s^{-1}) or shell inner diameter (m)
E	enhancement factor for chemical reaction
G	gas voluminal flow rate (m^3s^{-1}),
H	Henry's coefficient
Ha	Hatta number
J	mass-transfer flux ($mol\,m^{-2}s^{-1}$)
K	overall mass-transfer coefficient (ms^{-1})
k	individual mass-transfer coefficient (ms^{-1}), or reaction rate constant ($m^3\,mol^{-1}s^{-1}$ or s^{-1})
k_L°	physical mass transfer coefficient (s^{-1})
L	length of a hollow fiber (m)
n	fiber number of the module
P	pressure (MPa)
r	fiber radius (m or μm)
R	reaction rate ($mol\,m^{-3}s^{-1}$)
Re	Reynolds number
Sc	Schmidt number
Sh	Sherwood number
T	temperature (K)
u	velocity (ms^{-1})
V	flow rate (ms^{-1})
y	mole fraction of i in the gas phase
z	length of fiber (m)

Subscripts

a	alkanolamine
D	molecular diffusion
ext	external
G	glyine
g	gas phase
h	hydrodynamic
i	component (=CO_2)
in	inlet or inner
int	interface
K	Knudsen diffusion
L	liquid phase
P	piperazine
m	membrane phase
mem	membrane
o	outer
out	outlet
ov	overall
z	z axis

Greek Letters

α	liquid CO_2-loading (mol/mol)
δ	thickness of membrane wall (m or μm)
ε	porosity
φ	packing fraction
η	capture efficiency
μ	viscosity (Pa s)
τ	tortuosity of the membrane pore

REFERENCES

1. Herzog, H.; Eliasson, B.; Kaarstad, O. (2000) Capturing greenhouse gases. *Sci. Am.*, 182 (2): 72–79.
2. Houghton, R.A.; Hachler, J.L.; Lawrence, K.T. (1999) The U.S. Carbon budget: Contributions from land use change. *Science*, 285: 574–578.
3. Rao, A.B.; Rubin, E.S. (2002) A technical, economic, and environmental assessment of amine-based CO_2 capture technology for power plant greenhouse gas control. *Environ. Sci. Technol.*, 36: 4467–4475.
4. Granite, E.J.; O'Brien, T. (2005) Review of novel methods for carbon dioxide separation from flue and fuel gases. *Fuel Process. Technol.*, 86: 1423–1434.
5. Gabelman, A.; Hwang, S.T. (1999) Hollow fiber membrane contactors. *J. Membr. Sci.*, 159: 61–106.
6. Lia, L.-L.; Chen, B.-H. (2005) Review of CO_2 absorption using chemical solvents in hollow fiber membrane contactors. *Sep. Purif. Technol.*, 41: 109–122.
7. Zhang, Q.; Cussler, E.L. (1985) Microporous hollow fibers for gas absorption. *J. Membr. Sci.*, 23: 321–345.
8. Kumar, P.S.; Hogendoorn, J.A.; Feron, P.H.M.; Versteeg, G.F. (2002) New absorption liquids for the removal of CO_2 from dilute gas streams using membrane contactors. *Chem. Eng. Sci.*, 57: 1639–1651.
9. Wang, R.; Li, D.F.; Liang, D.T. (2004) Modeling of CO_2 capture by three typical amine solutions in hollow fiber membrane contactors. *Chem. Eng. Process.*, 43: 849–856.
10. Dindore, V.Y.; Brilman, D.W.F.; Feron, P.H.M.; Versteeg, G.F. (2004) Membrane solvent selection for CO_2 removal using membrane gas–liquid contactors. *J. Membr. Sci.*, 235: 99–109.
11. Lu, J.-G.; Wang, L.-J.; Sun, X.-Y.; Li, J.-S.; Liu, X.-D. (2005) Absorption of CO_2 into aqueous solutions of methyldiethanolamine and activated methyldiethanolamine from a gas mixture in a hollow fiber contactor. *Ind. Eng. Chem. Res.*, 44: 9230–9238.
12. Zhang, H.-Y.; Wang, R.; Liang, D.T.; Tay, J.H. (2006) Modeling and experimental study of CO_2 absorption in a hollow fiber membrane contactor. *J. Membr. Sci.*, 279: 301–310.
13. Gong, Y.; Wang, Z.; Wang, S.-C. (2006) Experiments and simulation of CO_2 removal by mixed amines in a hollow fiber membrane module. *Chem. Eng. Process.*, 45: 652–660.
14. Lu, J.-G.; Zheng, Y.-F.; Cheng, M.-D.; Wang, L.-J. (2007) Effects of activators on mass-transfer enhancement in a hollow fiber contactor using activated alkanolamine solutions. *J. Membr. Sci.*, 289: 138–149.
15. Lu, J.-G.; Zheng, Y.-F.; Cheng, M.-D. (2008) Wetting mechanism in mass transfer process of hydrophobic membrane gas absorption. *J. Membr. Sci.*, 308: 180–190.
16. Hua, L.Q.; Shuo, Y.; Lin, T.J. (1999) A new complex absorbent used for improving propylene carbonate absorbent for carbon dioxide removal. *Sep. Purif. Technol.*, 16: 133–138.

17. Liao, C.H.; Li, M.H. (2002) Kinetics of absorption of carbon dioxide into aqueous solutions of monoethanolamine + N-methyldiethanolamine. *Chem. Eng. Sci.*, 57: 4569–4582.
18. Paul, S.; Ghoshal, A.K.; Mandal, B. (2008) Theoretical studies on separation of CO_2 by single and blended aqueous alkanolamine solvents in flat sheet membrane contactor (FSMC). *Chem. Eng. J.*, 144: 352–360.
19. Tim Cullinane, J.; Rochelle Gary, T. (2004) Carbon dioxide absorption with aqueous potassium carbonate promoted by piperazine. *Chem. Eng. Sci.*, 59: 3619–3630.
20. Caplow, M. (1968) Kinetics of carbamate formation and breakdown. *J. Am. Chem. Soc.*, 90: 6795–6803.
21. Xu, G.-W.; Zhang, C.-F.; Qin, S.-J.; Wang, Y.-W. (1992) Kinetics study on absorption of carbon dioxide into solutions of activated methydiethanolamine. *Ind. Eng. Chem. Res.*, 31: 921–926.
22. Zhang, X.; Zhang, C.-F.; Qin, S.-J.; Zheng, Z.-S. (2001) A kinetics study on the absorption of carbon dioxide into a mixed aqueous solution of methyldiethanolamine and piperazine. *Ind. Eng. Chem. Res.*, 40: 3785–3791.
23. Sun, W.-Ch.; Yong, Ch.-B.; Li, M.-H. (2005) Kinetics of the absorption of carbon dioxide into mixed aqueous solutions of 2-amino-2-methyl-l-propanol and piperazine. *Chem. Eng. Sci.*, 60: 503–516.
24. Portugal, A.F.; Derks, P.W.J.; Versteeg, G.F.; Magalhaes, F.D.; Mendes, A. (2007) Characterization of potassium glycinate for carbon dioxide absorption purposes. *Chem. Eng. Sci.*, 62: 6534–6547.
25. Samanta, A.; Bandyopadhyay, S.S. (2007) Kinetics and modeling of carbon dioxide absorption into aqueous solutions of piperazine. *Chem. Eng. Sci.*, 62: 7312–7319.
26. Pinsent, B.R.W.; Pearson, L.; Roughton, F.W.J. (1956) The kinetics of combination of carbon dioxide with hydroxide ions. *Transactions of Faraday Society*, 52: 1512–1520.
27. Zhang, Q.; Cussler, E.L. (1985) Microporous hollow fibers for gas absorption: II. Mass transfer across the membrane. *J. Membr. Sci.*, 23: 333–345.
28. Prasad, R.; Sirkar, K.K. (1988) Dispersion free solvent extraction with microporous hollow-fiber modules. *AIChE J.*, 34: 177–188.
29. Haimour, N.; Bidarian, A.; Sandall, O.C. (1987) Kinetics of the reaction between carbon dioxide and methyldiethanolamine. *Chem. Eng. Sci.*, 42: 1393.
30. DeCoursey, W.J. (1982) Enhancement factor for gas absorption with reversible chemical reaction. *Chem. Eng. Sci.*, 37: 1483–1489.
31. Kumar, P.S.; A Hogendoorn, J.; Feron, P.H.M.; Versteeg, G.F. (2003) Approximate solution to predict the enhancement factor for the reactive absorption of a gas in a liquid flowing through a microscopic membrane hollow fiber. *J. Membr. Sci.*, 213: 231–245.
32. Wilke, C.R.; Chang, P. (1955) Correlation of diffusion coefficients in dilute solutions. *AIChE J.*, 1: 264–270.
33. Skelland, A.H.P. (1974) *Diffusional Mass Transfer*; Wiley: New York.
34. Versteeg, G.F.; van Swaaij, W.P.M. (1988) Solubility and diffusivity of acid gases (CO_2, N_2O) in aqueous alkanolamine solutions. *J. Chem. Eng. Data*, 33: 29–34.
35. Bensetiti, Z.; Iliuta, I.; Larachi, F.; Grandjean, B.P.A. (1999) Solubility of nitrous oxide in amine solutions. *Ind. Eng. Chem. Res.*, 38: 328–332.
36. Weisenberger, S.; Schumpe, A. (1996). Estimation of gas solubilities in salt solutions at temperatures from 273 K to 363 K. *AIChE. J.*, 42: 298–300.
37. Mandal, B.P.; Biswas, A.K.; Bandyopadhyay, S.S. (2003) Absorption of carbon dioxide into aqueous blends of 2-amino-2-methyl-1-propanol and diethanolamine. *Chem. Eng. Sci.*, 58: 4137–4144.
38. Dindore, V.Y.; Brilman, D.W.F.; Versteeg, G.F. (2005) Modelling of cross-flow membrane contactors: Mass transfer with chemical reactions. *J. Membr. Sci.*, 255: 275–289.
39. Kumar, P.S.; Hogendoorn, J.A.; Feron, P.H.M.; Versteeg, G.F. (2003) Equilibrium solubility of CO_2 in aqueous potassium taurate solutions: Part 1. Crystallization in carbon dioxide loaded aqueous salt solutions of amino acids. *Ind. Eng. Chem. Res.*, 42: 2832–2840.
40. Garcia-Payo, M.C.; Izquierdo-Gil, M.A.; Fernandez-Pineda, C. (2000) Wetting study of hydrophobic membranes via liquid entry pressure measurements with aqueous alcohol solutions. *J. Colloid Interf. Sci.*, 230: 420–431.